Med Chem Res
DOI 10.1007/s00044-017-1931-9

MEDICINAL CHEMISTRY RESEARCH

ORIGINAL RESEARCH

Synthesis, spectral characterization, DNA binding ability and anti-cancer screening of new acridine-based derivatives

Othman M. Salem[1] · Mária Vilková[2] · Jana Janočková[1,3] · Rastislav Jendželovský[4] · Peter Fedoročko[4] · Ján Imrich[2] · Mária Kožurková[1,3]

Received: 4 March 2016 / Accepted: 22 May 2017
© Springer Science+Business Media New York 2017

Abstract In this study, a series of newly synthesized acridine derivatives, compounds **4**, **6a**, and **6b**, are described and their biological activity on HL-60 cell lines is assessed using a number of different techniques. Binding studies were also performed between the derivatives and DNA in order to characterize the mechanism of the agents' effect in more detail. The results of ultraviolet–visible absorption spectroscopy prove that the binding of derivatives **4**, **6a**, and **6b** had occurred with a binding constant value of $K = 3.5 \times 10^4$–$4.0 \times 10^4\ M^{-1}$. These findings are indicative of a strong interaction between the derivatives and DNA, and this hypothesis is supported by the results of the fluorescence emission, linear dichroism, and viscometric assays.

Keywords Acridine derivatives · Topoisomerases I and II · HL-60 cells · DNA binding

✉ Mária Kožurková
maria.kozurkova@upjs.sk

[1] Department of Biochemistry, P. J. Šafárik University, Košice, Slovakia

[2] Department of Organic Chemistry, Institute of Chemistry, P. J. Šafárik University, Košice, Slovakia

[3] Biomedical Research Center, University Hospital Hradec Kralove, Hradec Kralove, Czech Republic

[4] Department of Cellular Biology, Faculty of Science, Institute of Biology and Ecology, P. J. Šafárik University, Košice, Slovakia

Introduction

As the costs of testing and licensing new drugs continue to rise, there is a growing trend among researchers of reinvestigating and improving drugs that are already in the market. One example of a widely available drug group that could be reassessed in this manner would be acridine derivatives. These compounds form one of the best-known classes of multi-target anti-cancer agents, and the drugs operate by interfering with DNA synthesis and inhibiting topoisomerases. A fuller understanding of acridine derivatives would be of considerable interest in our work in the development DNA topoisomerase inhibitors as chemotherapeutic agents (Vantova et al. 2009; Janočková et al. 2015a, b; Salem et al. 2015, 2016). The dynamic nature of the DNA molecule permits essential biological functions such as replication, transcription, recombination, repair and DNA segregation, and topoisomerase enzymes regulate these topological changes by introducing or removing supercoiling, knots, or catenations in DNA molecules (Champoux 2001; Vos et al. 2011; Yao et al. 2015). DNA is generally the primary intracellular target of anti-cancer drugs, so the interaction between small molecules and DNA can cause DNA damage in cancer cells and block the division of cancer cells, thereby resulting in cell death. As cancer cells exhibit high levels of topoisomerase activity and demonstrate remarkable sensitivity to DNA-targeted drugs, a large number of anti-cancer drugs have been designed and synthesized that specifically target the interaction between DNA and topoisomerases (Lafayette et al. 2013; Lang et al. 2013; Li et al. 2014). Despite the side effects associated with DNA-targeted compounds, topoisomerase inhibitors are still recognized as being the main drug of choice in prolonging the lives of patients, but these agents are unfortunately accompanied by a number of side

Published online: 12 June 2017

effects. Therefore, research into novel DNA-binding agents that act as topoisomerase inhibitors remains a high priority in the fight against cancer (Rajendran and Nair 2006; Di Giorgio et al. 2008; Goodell et al. 2008; Moukharskaya and Verschraegen 2012; Barros et al. 2012, 2013).

Our work focuses on the development of novel acridine derivatives that possess bioactive heterocyclic substituents, which are able to interact or interfere with cell processes or metabolites. We also aim to produce new approaches and techniques for the synthesis and preparation of such agents that would be attractive and viable from a chemical point of view. As a continuation of our research interest (Ungvarská Maľučká et al. 2016) in the chemical transformation of acridine moiety, we decided to investigate other carbon–carbon double-bond forming reactions. In this study, we synthesize and describe three new acridine derivatives that possess a biologically active CH=CH moiety, a feature that would be expected to demonstrate some degree of anti-cancer activity. The biochemical and biological activities of acridine derivatives **4**, **6a**, and **6b** were tested in order to examine their capacity to bind to DNA and to interfere with calf thymus topo I. The binding constants of these dyes with calf thymus DNA (ctDNA) were determined using ultraviolet–visible (UV–Vis) measurements and these results will be presented as an approach to the investigation of in vivo interactions. Linear dichroism (LD) spectroscopy, viscosity measurement, and DNA melting studies were also performed in order to obtain a deeper insight into the DNA-binding affinity of these novel derivatives. The biological activity of the novel compounds were assessed using a number of techniques, which include examinations of cell cycle distribution and changes in the mitochondrial membrane potential (MMP) in HL-60 cell lines.

Materials and methods

Chemistry

General information and materials

Nuclear magnetic resonance (NMR) spectra were recorded at room temperature on a Varian VNMRS spectrometer operating at 599.87 MHz for ^{1}H, 150.84 MHz for ^{13}C, and 60.79 MHz for ^{15}N. Spectra were recorded in $CDCl_3$ or DMSO-d_6 and the chemical shifts were referenced to the residual solvent signal ($CDCl_3$: ^{1}H NMR 7.26 ppm, ^{13}C NMR 77.0 ppm; DMSO-d_6: ^{1}H NMR 2.50 ppm, ^{13}C NMR 39.5 ppm). 2D gCOSY, gHSQC, gHMBC (optimized for a long-range coupling of 8 Hz) methods were employed (Vilková et al. 2016). Melting points were determined on a Boetius hot-stage apparatus and are uncorrected. Elemental analysis was performed on a Perkin Elmer CHN 2400 elemental analyzer.

All purchased chemical were of reagent grade and used without further purification. Ethidium bromide (EB), dimethyl sulfoxide (DMSO), ctDNA, propidium iodide (PI), EB and tetramethylrhodamine ethyl ester (TMRE), plasmid pUC 19 (2761 bp, *DH* 5α), agarose (type II No-A-6877) were obtained from Sigma-Aldrich Chemie (Germany); EDTA, RNase A, and proteinase K were purchased from Serva (Germany); fluorescein diacetate (FDA) from BD Pharmingen (USA); RPMI-1640 medium, penicillin, streptomycin, amphotericin, fetal bovine serum from Gibco (Invitrogen, USA); and all other chemicals were purchased from Lachema (the Czech Republic). HL-60 cell lines were purchased from American Type Culture Collection (ATCC, USA).

Synthesis of (2E)-3-(acridin-9-yl)prop-2-enoic acid (**2**) A solution of sodium hydroxide (2 equiv) was added to a solution of methyl (2*E*)-3-(acridin-9-yl)prop-2-enoate (**1**, 500 mg, 1.90 mmol) in methanol (10 mL). After stirring for 8 h, the solvent was evaporated in vacuo. The reaction was quenched by the addition of water (25 mL). The aqueous portion was acidified to pH 2 with 6 M hydrochloric acid. The carboxylic acid was precipitated on standing, filtered off, and dried (Vilková et al. 2016).

Yield 420 mg, 89%. Mp 225–226 °C. Bright yellow solid. [Found: C 77.21; H 4.22; N 5.49; $C_{16}H_{11}NO_2$ (249.269) requires C 77.10; H 4.45; N 5.62%]. ^{1}H NMR (600 MHz, DMSO-d_6): 8.14 (1H, d, *J* 16.8, H-3), 8.19 (2H, dd, *J* 7.2, H-1′,8′), 8.18 (2H, dd, *J* 7.2, H-4′,5′), 7.88 (2H, ddd, *J* 6.6, 1.2, H-3′,6′), 7.66 (2H, ddd, *J* 8.4, H-2′,7′), 6.43 (1H, d, *J* 16.2, H-2); ^{13}C NMR (150 MHz, DMSO-d_6): 166.8 (C-1), 148.5 (C-4′a,10′a), 140.7 (C-9′), 138.5 (C-3), 131.0 (C-2), 130.9 (C-3′,6′), 130.0 (C-4′,5′), 127.1 (C-2′,7′), 125.9 (C-1′,8′), 123.6 (C-8′a,9′a) ppm.

Synthesis of (2E)-3-(acridin-9-yl)prop-2-enoyl chloride (**3**) The acid chloride was prepared through the reaction of carboxylic acid **2** (500 mg, 2.00 mmol) and thionyl chloride (480 mg, 4.03 mmol) in freshly distilled dichloromethane (10 mL) by heating under reflux for 8 h. The excess of thionyl chloride was removed under reduced pressure and the resulting product was used in the next step without further purification (Ilis et al. 2011).

Yield 480 mg, 88%. ^{1}H NMR (600 MHz, DMSO-d_6): 8.59 (2H, d, *J* 9.0, H-4′,5′), 8.56 (1H, d, *J* 16.2, H-3), 8.48 (2H, d, *J* 7.2, H-1′,8′), 8.30 (2H, t, *J* 7.2, H-3′,6′), 7.94 (2H, t, *J* 7.2, H-2′,7′), 6.58 (1H, d, *J* 16.2, H-2); ^{13}C NMR (150 MHz, DMSO-d_6): 165.6 (C-1), 151.9 (C-9′), 140.1 (C-4′a,10′a), 136.2 (C-3), 136.1 (C-3′,6′), 133.1 (C-2), 128.0 (C-2′,7′), 127.0 (C-1′,8′), 123.6 (C-8′a,9′a), 121.1 (C-4′,5′) ppm.

Synthesis of propyl (2E)-3-(acridin-9-yl)prop-2-enoate (**4**) (*E*)-3-(acridin-9-yl)propenoyl chloride (**3**, 1 equiv) was added to a stirred cooled dichloromethane solution (0 °C, 1 mL) of triethylamine (2 equiv) and ethanol (5 equiv). After stirring for 24 h at room temperature, the reaction mixture was then concentrated in vacuo, and the residue was purified by column chromatography on silica gel (1:1 hexane-ethyl acetate) to produce ester **4**.

Yield 70 mg, 65%. Bright yellow solid. Mp 179−180 °C. [Found: C 78.21; H 5.66; N 4.65; $C_{19}H_{17}NO_2$ (291.349) requires C 78.33; H 5.88; N 4.81%]. ^{1}H NMR (600 MHz, $CDCl_3$): 8.54 (1H, d, *J* 16.2, H-3), 8.29 (2H, d, *J* 9.0, H-4′,5′), 8.19 (2H, d, *J* 8.4, H-1′,8′), 7.81 (2H, t, *J* 9.0, 7.8, H-3′,6′), 7.58 (2H, t, *J* 8.4, 7.8, H-2′,7′), 6.48 (1H, d, *J* 16.2, H-2), 4.30 (2H, t, *J* 14.1, H-1″), 1.82 (2H, k, *J* 14.1, 7.2, H-2″), 1.05 (3H, t, *J* 7.2, H-3″); ^{13}C NMR (150 MHz, $CDCl_3$): 165.7 (C-1), 148.0 (C-4′a,10′a), 140.4 (C-9′), 139.0 (C-3), 130.5 (C-3′,6′), 129.6 (C-2, C-4′,5′), 126.5 (C-2′,7′), 125.2 (C-1′,8′), 123.8 (C-8′a,9′a), 66.8 (C-1″), 22.1 (C-2″), 10.5 (C-3″) ppm.

General procedure for the synthesis of 9-[(E)-2-(nitrophenyl)ethenyl]acridine ***6a, b***

A mixture of 9-methylacridine (**5**) (1.0 g, 5.17 mmol), appropriate aldehyde (0.782 g, 5.17 mmol), and zinc chloride (0.776 g, 5.70 mmol) was heated at 130 °C for 3 h. The reaction mixture was cooled to room temperature and was partitioned between aqueous sodium hydroxide and chloroform. The organic phase was washed with water and brine, dried over magnesium sulfate, filtered, and concentrated in vacuo. The residue was purified by silica gel column chromatography (4:1 hexane-acetone) to produce compound **6** (Tsukamoto et al. 2009).

9-[(E)-2-(4-nitrophenyl)ethenyl]acridine (**6a**) Yield 1.12 mg, 66%. Bright yellow solid. Mp 286−287 °C. [Found: C 77.17; H 4.25; N 8.34; $C_{21}H_{14}N_2O_2$ (326.354) requires C 77.29; H 4.32; N 8.58%]; ^{1}H (600 MHz, DMSO-d_6): 8.49 (1H, d, *J* 16.2, H-2), 8.41 (2H, d, *J* 9.0, H-1′,8′), 8.34 (2H, d, *J* 8.7, H-3″,5″), 8.20 (2H, d, *J* 8.5, H-4′,5′), 8.16 (2H, d, *J* 8.7, H-2″,6″), 7.89 (2H, ddd, *J* 8.8, 6.5, 1.4, H-3′,6′), 7.66 (2H, ddd, *J* 8.9, 6.5, 1.3, H-2′,7′), 7.32 (1H, d, *J* 16.6, H-1); ^{13}C (150 MHz, DMSO-d_6): 148.2 (C-4′a,10′a), 147.0 (C-4″), 142.9 (C-1″), 141.9 (C-9′), 137.3 (C-1), 130.3 (C-3′,6′), 129.6 (C-4′,5′), 128.3 (C-2″,6″), 127.2 (C-2), 126.2 (C-2′,7′), 125.9 (C-1′,8′), 124.0 (C-3″,5″), 123.6 (C-8′a,9′a); ^{15}N (61 MHz, DMSO-d_6): −74.4 (N-10′), −9.8 (NO_2) ppm.

9-[(E)-2-(3-nitrophenyl)ethenyl]acridine (**6b**) Yield 1.38 g, 82%. Bright yellow solid. Mp 208−209 °C. [Found: C 77.15; H 4.14; N 8.29; $C_{21}H_{14}N_2O_2$ (326.354) requires C 77.29; H 4.32; N 8.58%]; ^{1}H (600 MHz, DMSO-d_6): 8.72 (1H, t, *J* 2.0, H-2″), 8.45 (1H, d, *J* 17.0, H-2), 8.43 (2H, d, *J* 8.5, H-1′,8′), 8.37 (1H, d, *J* 7.8, H-6″), 8.25 (1H, dd, *J* 8.2, 2.4, H-4″), 8.19 (2H, d, *J* 8.7, H-4′,5′), 7.88 (2H, ddd, *J* 8.8, 6.5, 1.3, H-3′,6′), 7.78 (1H, t, *J* 8.0, H-5″), 7.65 (2H, ddd, *J* 8.8, 6.5, 1.3, H-2′,7′), 7.31 (1H, d, *J* 16.7, H-1); ^{13}C (150 MHz, DMSO-d_6): 148.4 (C-3″), 148.2 (C-4′a,10′a), 142.2 (C-9′), 138.2 (C-1″), 137.1 (C-1), 133.3 (C-6″), 130.3 (C-6′), 130.2 (C-5″), 129.5 (C-4′,5′), 126.1 (C-1′,8′; C-2′,7′), 125.4 (C-2), 123.7 (C-8′a,9′a), 123.0 (C-4″), 121.8 (C-2″); ^{15}N (61 MHz, DMSO-d_6): −75.1 (N-10′), −9.3 (NO_2) ppm.

The novel acridine derivatives **4**, **6a**, and **6b** were dissolved in absolute DMSO at a concentration of 5×10^{-3} M. The solutions were stored in darkness at 4 °C. A stock solution of ctDNA was prepared in a TE buffer (pH = 7.4). The concentrations of the DNA samples per mole phosphate were determined spectrophotometrically at 260 nm using a molar extinction coefficient of 6600 cm^{-1} M^{-1}.

UV–Vis spectroscopic studies

UV–Vis spectra were obtained using a Varian Cary 100 UV–Vis spectrophotometer in a pH 7.4 buffer at room temperature using 1 × 1 cm quartz cuvettes. The UV–Vis spectra of compounds **4**, **6a**, and **6b** and compounds–ctDNA complexes were recorded at a wavelength range of 200−600 nm, in a 10 mM Tris-HCl buffer, pH 7.4. Experiments were carried out in with fixed concentrations of derivatives **4**, **6a**, and **6b** (6.25×10^{-5} M) and varying concentrations of DNA (0–31×10^{-4} M).

Thermal denaturation

Thermal studies were carried out using a Varian Cary Eclipse spectrophotometer, equipped with a temperature controlling programmer (±0.1 °C). The absorbance at 260 nm was continuously monitored (10 mM Tris-HCl buffer, pH 7.4) for solutions of ctDNA (3.2×10^{-3} M) in the absence and presence of the complexes (7.5×10^{-6} M). The temperature of the solution was increased by 0.4 °C min^{-1}.

Equilibrium binding titration

The binding affinities were calculated from absorbance spectra according to the McGhee and von Hippel method using data from a Scatchard plot (McGhee and von Hippel 1974; Jenkins 1997). The binding data were fitted using GNU Octave 2.1.73 software (Busa 2006).

Fluorescence measurements

Fluorescence spectra were recorded at room temperature at a range of 520–800 nm with an excitation wavelength at 500 nm. The widths of both the excitation and emission slits were set at 10 nm. The intercalating effect of derivatives **4**, **6a**, and **6b** (1.2×10^{-4} M) with the ctDNA–EB complex was studied by adding specific quantities of the compound into the quartz cuvette containing a fixed concentration of the ctDNA–EB complex solution. The concentration of EB was 6.0×10^{-5} M, while that of the ctDNA was 1.0×10^{-6} M. The influence of the addition of each compound to the DNA–EB complex solution was observed by recording variations in the fluorescence emission spectra.

LD spectroscopy

Flow LD spectra were collected by using a flow Couette cell in a Jasco J-720 spectropolarimeter adapted for LD measurements. It is possible to orient long molecules such as DNA (minimum length of ~250 bp) in a flow Couette cell. The flow cell consists of a fixed outer cylinder and a rotating solid quartz inner cylinder separated by a gap of 0.5 mm, giving a total pathlength of 1 mm. LD spectra of ctDNA at a concentration of 2.0×10^{-4} M modified by acridine derivatives **4**, **6a**, and **6b** ($0.79–3.96 \times 10^{-5}$ M) were recorded at 25 °C in a 10 mM Tris-HCl buffer (pH 7.4) in the range of 220–600 nm.

Viscometric measurements

Viscosity experiments were conducted on a AMVn Automated Micro Viscometer (Anton Paar GmbH, Austria) using a 1.6-mm capillary tube at constant temperature of 25 ± 0.1 °C. Titrations were performed by adding various concentrations of derivatives **4**, **6a**, and **6b** ($2.5–10 \times 10^{-5}$ M) to a ctDNA solution (1.6×10^{-3} M) which had been placed in the viscometer. Data were presented as $(\eta/\eta_0)^{1/3}$ vs. the ratio of the concentration of the compound to ctDNA, where η is the viscosity of ctDNA in the presence of the compound and η_0 is the viscosity of ctDNA in the absence of the compound. Viscosity values were calculated from the observed flow time of the DNA containing solutions (t) and corrected for buffer solution (t_0), $\eta = (t–t_0)/t_0$.

DNA topoisomerase I relaxation assay

The effects of the acridine derivatives on the relaxation of plasmid DNA with topoisomerase I were performed using the methods described previously by Janočková et al. (2015a, b). A plasmid pBR322 (1.4 µg) was incubated for 45 min at 37 °C with two units of calf thymus topoisomerase I (Takara, Japan) in both the absence and presence of the acridine derivatives (5, 30, 60, and 80 µM, respectively) and these observations were used to estimate the effect.

Cell culture conditions

HL-60 cell lines were purchased from ATCC. Cells were grown in a RPMI-1640 medium supplemented with fetal bovine serum and antibiotics (100 U mL^{-1} penicillin; 100 µg mL^{-1} streptomycin; 25 µg mL^{-1} amphotericin) at 37 °C, 95% humidity and in an atmosphere of 5% CO_2 (Janočková et al. 2015b). For the experiments, cells were seeded in 96-well plates (MTT assay) or in 6-well plates (MMP dissipation, viability, cell cycle) (Trasadingen, Switzerland) to which the acridine derivatives were added. The results were analyzed 48 and 72 h after the addition of the compounds. Acridine was used as a positive control.

MTT assay

The metabolic activity of cells was evaluated using a MTT (3-[4,5-dimethylthiazol-2-yl]-2,5-diphenyltetrazolium bromide) reduction assay. At scheduled time points (48 and 72 h) MTT (5 mg mL^{-1}) was added and the cells (1×10^4) were incubated for another 4 h at 37 °C. The reaction was stopped and formazan crystals were dissolved by the addition of 100 µL sodium dodecyl sulfate (10%). The absorbance was measured at 584 nm using a BMG FLUOstar Optima (BMG Labtechnologies GmbH, Germany). Results were evaluated as percentages of absorbance of the untreated control.

Detection of MMP dissipation, metabolic activity and viability

HL-60 cells (1×10^6) were treated with varying concentrations of the studied acridine derivatives ($10–50 \times 10^{-6}$ M) and with acridine ($2–10 \times 10^{-6}$ M) as a positive control. Detection of MMP dissipation, metabolic activity, and viability was performed as described by Janočková et al. (2015a). After 48 and 72 h, incubation cells were harvested using centrifugation (5 min, 24 °C, 800 rpm), washed once with Hank's balanced salt solution and stained with TMRE (0.1 µmol dm^{-3}) in the case of MMP dissipation detection or double staining with FDA (100 ng mL^{-1}) and PI (25 µg mL^{-1}) in the case of metabolic activity and viability detection. These experiments were examined using a BD FACS Calibur flow cytometer (Becton Dickinson, USA), and the results were analyzed using FlowJo software (TreeStar Inc., USA).

Cell cycle analysis

HL-60 cells (1×10^6) were treated with varying concentrations of the studied acridine derivatives ($10–50 \times 10^{-6}$ M) and with acridine ($2–10 \times 10^{-6}$ M) as a positive control for 48 and 72 h using the method described by Salem et al. (2016). HL-60 cells were analyzed using a BD FACSCalibur flow cytometer. ModFit 3.0 software (Verity Software House, USA) was used to generate DNA content frequency histograms and to quantify the number of cells in the individual cell cycle phases.

Statistical analysis

Each experiment was performed at least three times and the results were expressed as mean values ± SD. The *t*-test was used to determine the significance levels that are indicated in the legend to each particular figure as $p < 0.05$ (*), $p < 0.01$ (**), and $p < 0.001$ (***).

Results and discussion

Chemistry

The esterification of carboxylic acids and transesterification of esters have a wide range of academic and industrial applications (Ramalinga et al. 2002; Khan et al. 2003). While a variety of procedures exist for the transesterification of esters, these protocols are often hindered by the need for excess reagents and/or expensive catalysts, and the production process can also produce undesirable side products.

Therefore, we decided to synthesize a new compound, derivative **4**, using conditions that were simple, fast, and that did not require the use of catalysts. The synthetic strategies adopted in order to synthesize compound **4** under the above-mentioned conditions are depicted in Scheme 1. Ester **4** was synthesized by adapting methodologies that have been described in previous literature with some very minor modifications (Scheme 1) (Khurana et al. 2004; Ilis et al. 2011). The key intermediate, compound **3**, was prepared in an excellent yield in two consecutive steps. Methyl (*2E*)-3-(acridin-9-yl)prop-2-enoate (**1**) (Vilková et al. 2016) was first transformed to (*2E*)-3-(acridin-9-yl)prop-2-enoic acid (**2**) using basic hydrolysis with NaOH in methanol at room temperature to achieve a complete conversion over the course of 24 h.

Chloride **3** was prepared from carboxylic acid **2** and thionyl chloride, and was subsequently transformed to ester **4** with appropriate alcohol and trimethylamine at a good yield as a bright yellow solid product. The new compound was characterized using elemental analysis and 1D and 2D NMR spectroscopy. The results of the ^{1}H NMR spectral

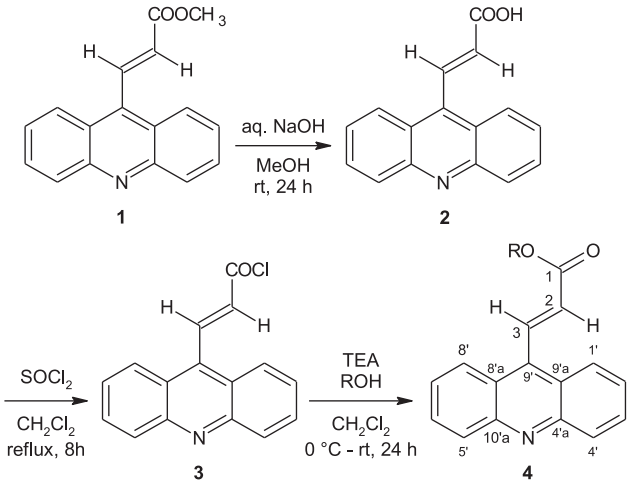

Scheme 1 Synthesis of propyl(*2E*)-3-(acridin-9-yl)prop-2-enoates **4**

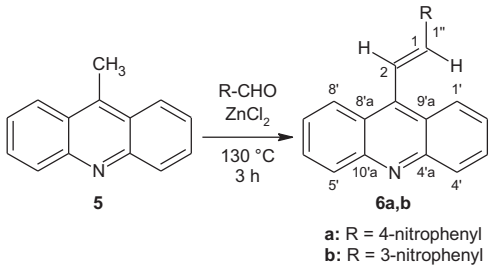

Scheme 2 Synthesis of 9-[(*E*)-2-(nitrophenyl)ethenyl]acridine **6a** and **6b**

data determined that the coupling constants between alkenic protons for derivative **4** had the value of 16.2 Hz, a value that confirms a *trans* (*E*) configuration of alkenes. These spectral data are consistent with those which have been reported previously (Vilková et al. 2016).

In a previously published study (Vilková et al. 2016), we described the synthesis of 9-(2-styryl)acridine from acridin-9-carbaldehyde using the Wittig reaction. However, on this occasion, we decided to synthesize 9-(2-styryl)acridine using the method described by Tsukamoto et al. (2009), which was simpler, faster, and which did not require the use of expensive catalysts. Following Tsukamoto's procedure, we carried out a condensation of 9-methylacridine (**5**) with 3- and 4-nitrobenzaldehyde under zinc chloride catalysis without a solvent to obtain 9-[(*E*)-2-(nitrophenyl)ethenyl] acridines (compounds **6a**, **6b**) (Scheme 2). Compounds **6a** and **6b** had an *E* configuration of the exocyclic double bond, as was determined from the presence of doublet signals in their ^{1}H NMR spectra due to olefinic protons at 7.31 (H-1) and 8.45 (H-2) ppm for derivative **6a** and 7.32 (H-1) and 8.49 (H-2) ppm for derivative **6b** with a coupling constant of approximately 16 Hz.

Absorption titration

The interaction of the newly synthesized **4**, **6a**, and **6b** derivatives (Schemes 1 and 2) with ctDNA was monitored using UV–Vis absorption spectroscopy. This procedure uses changes in the spectral observations to determine the existence of interaction between complexes and DNA and can also to define the mode of interaction that has occurred. In general, hypochromism may be detected in the case of intercalative binding of π–π^* stacking interactions (Li et al. 1997), while red shifts (bathochromism) are observed when the DNA duplex has been stabilized (Lang et al. 2013). The binding of derivatives **4**, **6a**, and **6b** complexes to DNA helices was determined by following the changes in absorbance and shifts in wavelength following each addition of DNA solution to the complex. The acridine derivative complexes in the DMSO-buffer mixture exhibited an intense transition in the region of 300–450 nm, a result which is suggestive of π–π^* intraligand transitions. A slight decrease in absorption and a small red shift were observed following the titration of ctDNA with complexes **4**, **6a**, and **6b**. The absorption spectra for compounds **4**, **6a**, and **6b** clearly show that the addition of DNA to the complexes produced hypochromism and a small red shift. These spectral characteristics strongly suggest that the interaction of the complexes with DNA involves stacking between the aromatic chromophore and the base pairs of DNA. The changes observed in the absorption spectra of ctDNA in the presence of complex **4** are given in Fig. 1. The results obtained from the UV–Vis titration experiments (Table 1) suggest that binding had occurred between the compounds and ctDNA, although it was not possible to determine the exact binding mode using UV–Vis spectroscopy alone. In most cases, the existence of hypochromism would be considered as convincing evidence of interaction between the base pairs of ctDNA, and this possibility cannot be ruled out. It is important to note that the planarity of ligands and their geometry play a significant role in the ability of the compounds to interact with DNA.

The binding constants, K, of the ligand–DNA complexes were calculated by integrating the variances in absorbance at the absorption band into McGhee and von Hippel plots. The calculated values of the binding constants K ranged from 3.6×10^4 to $4.0 \times 10^4\ M^{-1}$, and these results prove the strong affinity of the acridine ligands toward DNA and the calculated values also correspond to the range of binding constants which are characteristic for intercalators (10^4 to 10^6).

DNA melting is another important technique that is used to study the interaction of small molecules with nucleic acids. The thermal denaturation behavior of DNA in the presence of different complexes can give an insight into their conformational changes at increasing temperatures and offer information about the mode and strength of interaction of the complexes with DNA (Neyhart et al. 1993). Intercalative binding between DNA and small molecules can stabilize the DNA double-helical structure and this process increases the T_m by about 5–8 °C. However non-intercalative binding such as groove binding or electrostatic binding causes little or no perceptible increase in T_m. Denaturation of DNA is usually measured photometrically at the temperature-dependent extinction point at 260 nm. Table 1 shows that T_m of ctDNA was 66.02 °C and that ΔT_m

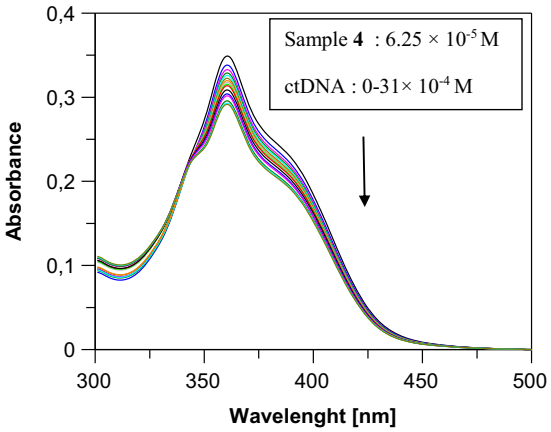

Fig. 1 UV–Vis absorption spectra of studied acridine derivatives (*upper line*, derivative **4**, 6.25×10^{-5} M) in the presence of increasing concentrations of ctDNA (*color lines*, 0–31×10^{-4} M, increment 2×10^{-4} M) in a 0.01 M Tris-HCl buffer (pH 7.4; 24 °C). *Arrow* indicates the absorption change upon increasing amounts of ctDNA

Table 1 UV–Vis absorption data of acridine derivatives **4**, **6a**, and **6b**

Compounds	λ_{max} free (nm)	λ_{max} bound (nm)	$\Delta\lambda$ (nm)	Hypochromicity (%)	$K \times 10^4$ (M^{-1})	T_m[a] (°C)	ΔT_m[a] (°C)	ΔG (kJ mol^{-1})
4	360	360	0	16.21	3.6	67.18	1.16	−19.59
6a	373	374	1	23.88	3.9	67.18	1.16	−19.39
6b	386	387	1	21.35	4.0	67.22	1.20	−19.32

[a] T_m measurements were performed in a Tris-HCl buffer (0.01 M), pH 7.4 using derivatives **4**, **6a**, and **6b** (7.5×10^{-6} M) and ctDNA (3.2×10^{-3} M) at a heating rate of 0.4 °C min^{-1}. T_m of ctDNA for measurement was 66.02 °C

increased from 0.84 to 1.16 °C in the presence of compounds **4**, **6a**, and **6b**. The high ΔT_m value for the complexes is suggestive of an intercalative mode of binding of complexes to DNA. In our case, only a slight shift increase in T_m was observed in the presence of the studied complexes in comparison with that recorded for free DNA. The small increase in DNA melting temperature in the presence of the complexes indicates that groove binding is the predominant mode of binding between the complexes and DNA (Kamatchi et al. 2013; Chitrapriya et al. 2011).

Fluorescence studies

In order to investigate the binding ability of studied derivatives and DNA in more detail, fluorescence absorption spectroscopy was employed. In the case of EB displacement assay, a solution containing a fixed concentration of EB and ctDNA was titrated with increasing concentrations of derivatives **4**, **6a**, and **6b**. EB–ctDNA complexes were excited at 500 nm and emission spectra were recorded from 520 to 800 nm. EB is a well-known intercalator that is often used as a spectral probe to estimate the binding mode of small molecules to double-helical DNA. The representative emission spectra of EB bound to DNA in both the absence and the presence of compounds **4**, **6a**, and **6b** are given in Fig. 2. If the titration of ctDNA-EB with compounds **4**, **6a**, and **6b** results in a decrease in fluorescence intensity, this would indicate that the studied derivatives compete with EB for interaction sites in DNA and dissociate EB from the system. As a consequence, derivatives **6a** and **6b** demonstrated a clear reduction in emission intensity, thereby suggesting that competitive binding interaction between derivatives **6a** and **6b** and EB with ctDNA had occurred, and also that derivatives **6a** and **6b** may interact with ctDNA mainly through an intercalative binding mode. Unlike derivatives **6a** and **6b**, derivative **4** showed a very slight reduction in emission spectra, indicating that this derivative had not displaced EB from the DNA–EB complex. These findings would suggest that derivative **4** is unlikely to interact with ctDNA through intercalation, and that any interaction is likely to be through an alternative mode of binding. However, not only the DNA intercalators but also groove DNA binders could cause the reduction in the emission intensities of DNA bound (Cain et al. 1978) but moderately for the latter case. For example, the non-intercalating DNA groove-binding agents of berenil, bisamidines, spermine, and spermidine were reported to be capable of displacing EB from DNA (Patel 1979).

Linear dichroism

LD measurements are often used to determine the orientation of ligands and their chromophores that are potentially

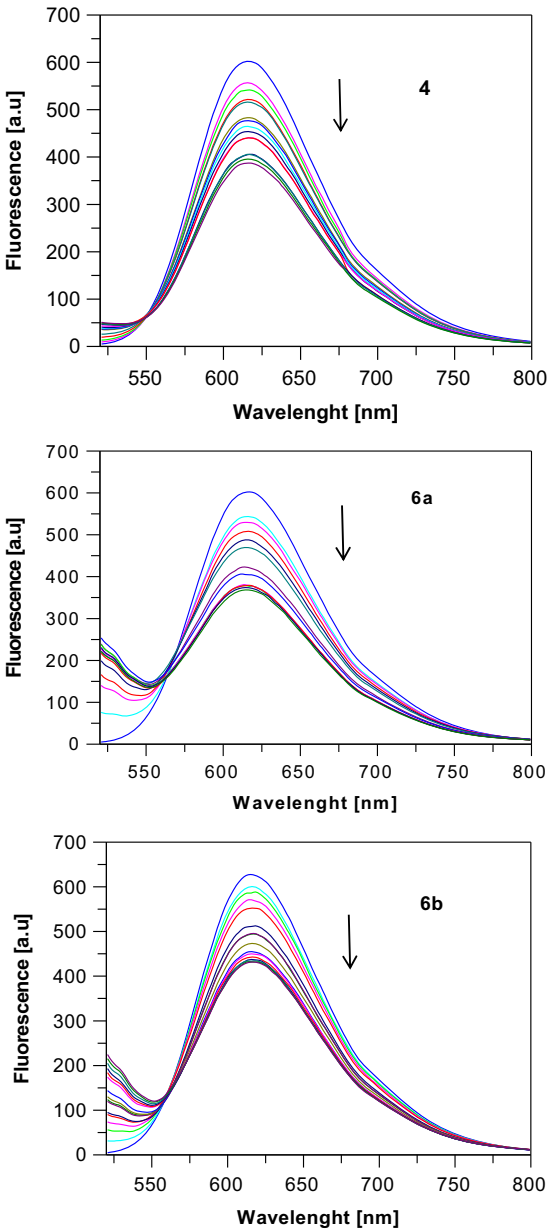

Fig. 2 Fluorescent displacement of EB (6.0×10^{-5} M, *black line*) bound to DNA (1.0×10^{-6} M) with increasing concentrations of derivatives **4**, **6a**, and **6b** (0–1.2×10^{-4} M), $\lambda_{ex} = 500$ nm, in a 0.01 M Tris-HCl (pH 7.4, 24 °C), corresponding to the curves from top to bottom, respectively

embedded into the DNA helical axis. Small molecules that are unbound or that are bound randomly to ctDNA are not oriented and show no signal. However, small molecules that are bound in a specific orientation with respect to ctDNA become oriented by the flow and their orientation shows a LD signal (Terenzi et al. 2013). The LD of these samples is characterized as the difference between the absorption of light polarized parallel ($A_{\parallel}$) and perpendicular ($A_{\perp}$) to the axis. LD measurements were also applied in order to investigate the DNA-binding mode of derivatives **4**, **6a**, and

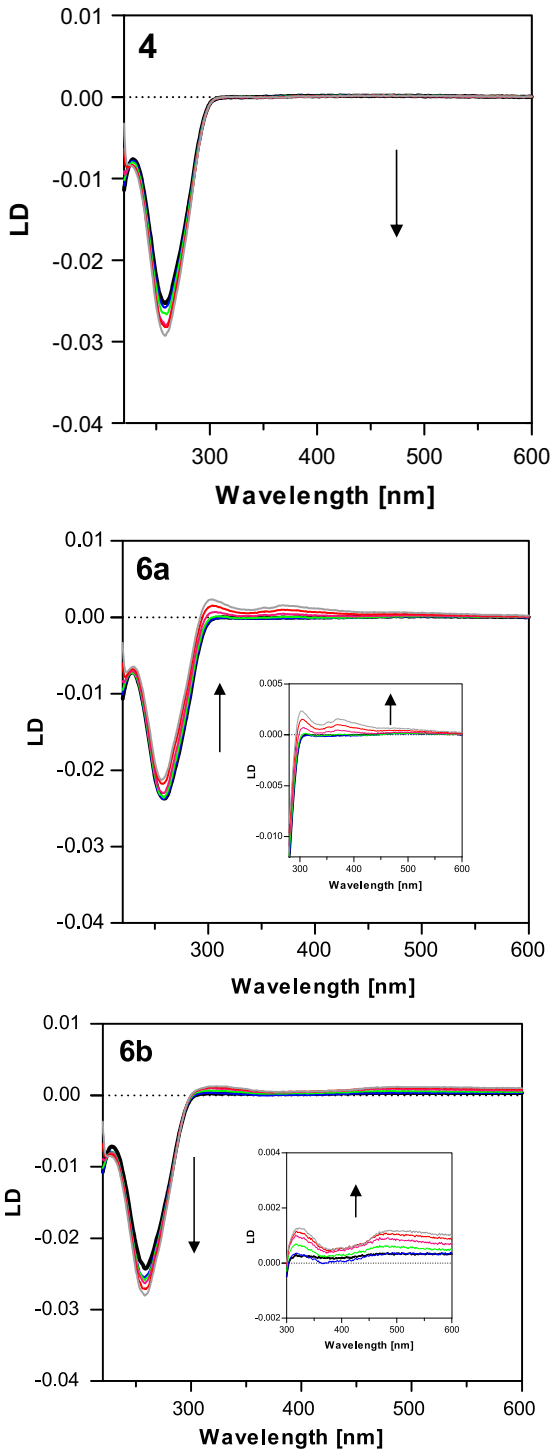

Fig. 3 LD spectra of ctDNA (2.0×10^{-4} M, *black line*) in the presence of increasing amounts of derivatives **4**, **6a**, and **6b** ($0.79–3.96 \times 10^{-5}$ M, *color line*) in a 0.01 M Tris-HCl solution (pH 7.4, 24 °C)

6b in more detail. The DNA base pairs are perpendicular to the helical axis, and ctDNA in its B-form demonstrates a representative negative band in the range of 220–300 nm, a finding which is likely the result of π–π* transitions within the bases. Ligands that are able to alter the structure of DNA can cause a decrease or increase of this band. Decreases in intensity could be connected to the bending or coiling potency of the ligands, while increases in intensity could be a result of intercalation, or the stiffening of the DNA. The LD spectra of ctDNA (2.0×10^{-4} M) in both the absence and presence of increasing concentrations of compounds **4**, **6a**, and **6b** ($0.79–3.96 \times 10^{-5}$ M) are presented in Fig. 3. The results show that compounds **4** and **6b** produced an increase in the intensity of the DNA negative band and that compound **6a** caused a decrease in the signal in this region. Moreover, the positive LD signals observed in the region of 300–600 nm suggest that compounds **6a** and **6b** bind to DNA in an oriented non-random fashion (Phelps et al. 2013).

Viscometry

In order to clarify the mode of binding of derivatives to ctDNA, viscosity measurements were also carried out using varying concentrations of derivatives **4**, **6a**, and **6b** in order to gather more information on the possible binding modes of the studied compounds and ctDNA. Intercalation binding typically causes an increase in the viscosity of the ligand–DNA complex because this form of binding requires a large space between adjacent base pairs in order to accommodate the ligand and lengthen the double helix (Hannon et al. 2001). In contrast, small molecules that bind exclusively in DNA grooves by partial or non-typical intercalation usually cause little or no change in the viscosity of the DNA solution (Ling et al. 2008; Rehman et al. 2014). The results obtained from the viscosity measurements of the ligand–ctDNA complex at increasing amounts of derivatives **4**, **6a**, and **6b** are presented in Fig. 4. No significant increase in the relative viscosity of ctDNA was observed at increasing concentrations of derivatives **4**, **6a**, and **6b**, and this suggests that derivatives **4**, **6a**, and **6b**

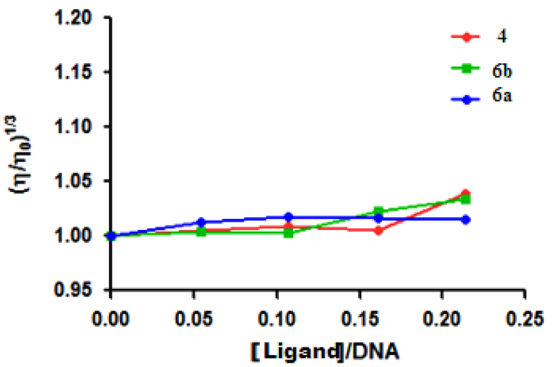

Fig. 4 Effect of increasing concentration of derivatives **4**, **6a**, and **6b** ($2.5–10 \times 10^{-5}$ M) on the viscosity of ctDNA. Concentration of ctDNA was constant (1.6×10^{-3} M) while the concentration of derivatives **4**, **6a**, and **6b** varied (0.01 M Tris-HCl buffer, pH 7.4; 24 °C)

prefer to interact with DNA through non-intercalative binding modes.

DNA topoisomerase I inhibition assay

In order to establish whether our newly synthesized derivatives possess the ability to inhibit topo I, a relaxation assay was performed using derivatives **4**, **6a**, and **6b** and plasmid pBR322 DNA mediated by topo I. As can be seen in Fig. 5, the supercoiled pBR322 DNA was fully relaxed by the enzyme in the absence of the studied derivatives (lane pBR322 + topo I). Derivatives **4**, **6a**, and **6b** demonstrated topo I inhibitory activity at 60 µM, with the exception of derivative **6a** which partially inhibited the activity of topo I at a concentration of 30 µM. All of these results indicate that these derivatives show some evidence of interaction with DNA and the inhibition of topo I, which in turn suggests that the compounds could be potential

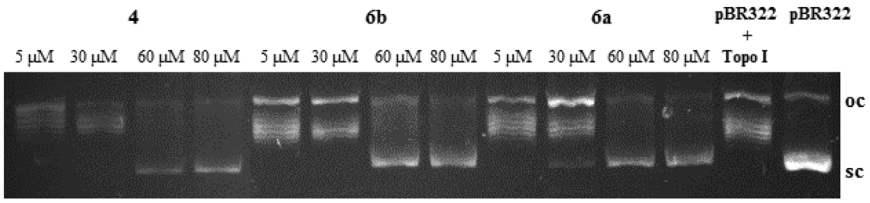

Fig. 5 Effect of the compounds on the relaxation of plasmid DNA by human topoisomerase I. pBR322 (Lane pBR322) was incubated with topo I (lane pBR322 + topo I) and studied compounds **4**, **6a** and **6b** (5, 30, 60, and 80 µM) 45 min at 37 °C. The DNA samples were run on agarose gel followed by EB staining. *Sc* supercoiled plasmid, *oc* open circular plasmid

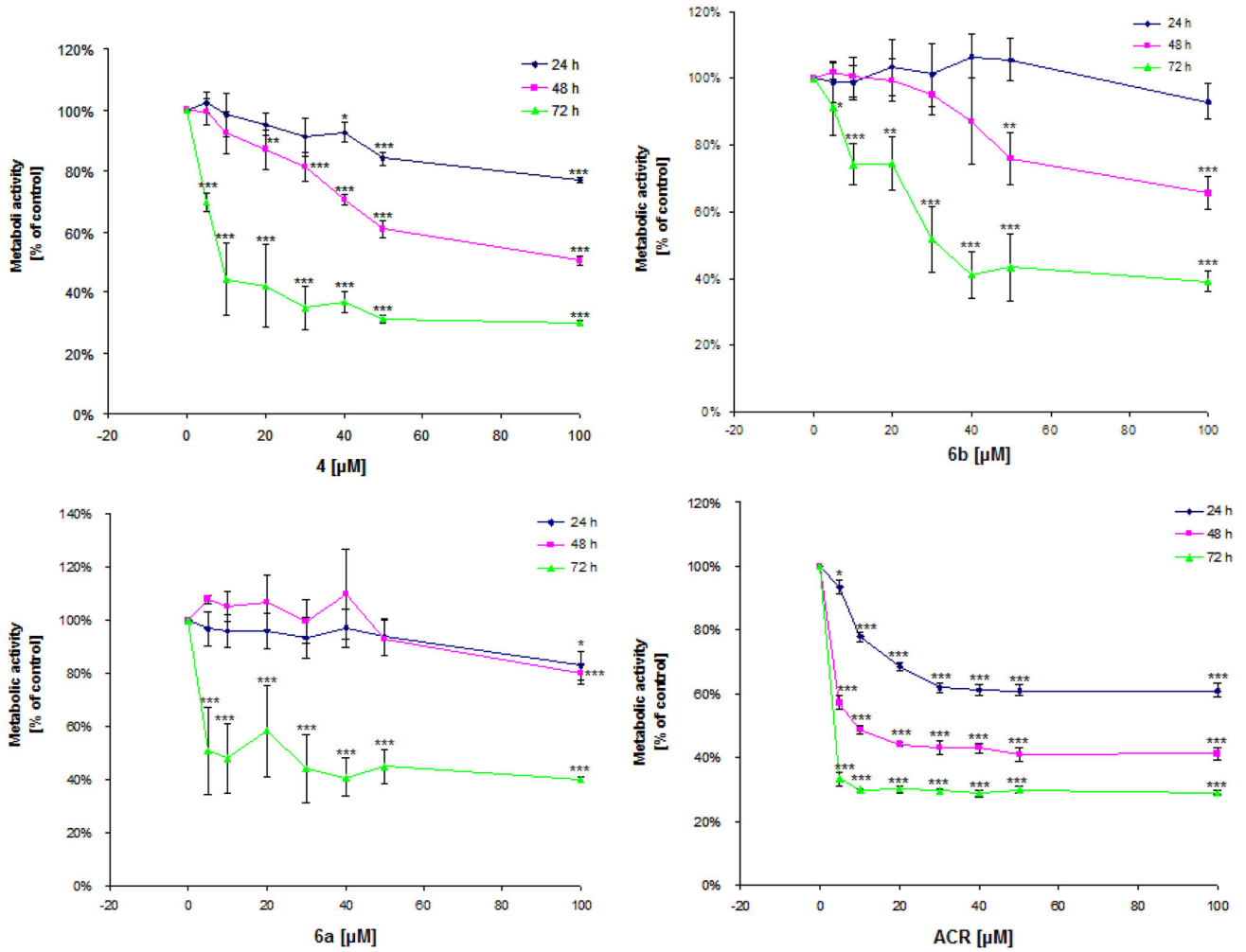

Fig. 6 MTT assay: effect of derivatives **4**, **6a**, and **6b** and acridine (ACR) (0–100 × 10^{-6} M) on the metabolic activity of HL-60 cells at 24, 48, and 72 h after treatment

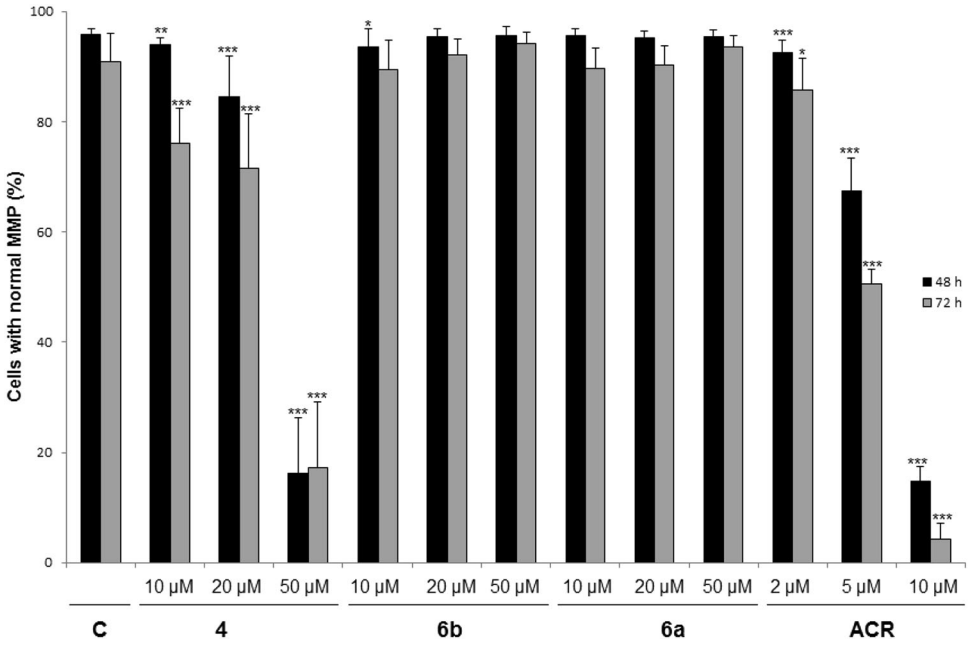

Fig. 7 The effect of acridine (ACR, positive control, 2–10 × 10^{-6} M) and derivatives **4**, **6a**, and **6b** (10–50 × 10^{-6} M) on changes in MMP 48 and 72 h after treatment. The results are presented as a mean ± SD, statistical significance: $p < 0.05$ (*), $p < 0.01$ (**), $p < 0.005$ (***) for particular experimental group compared to untreated control (C)

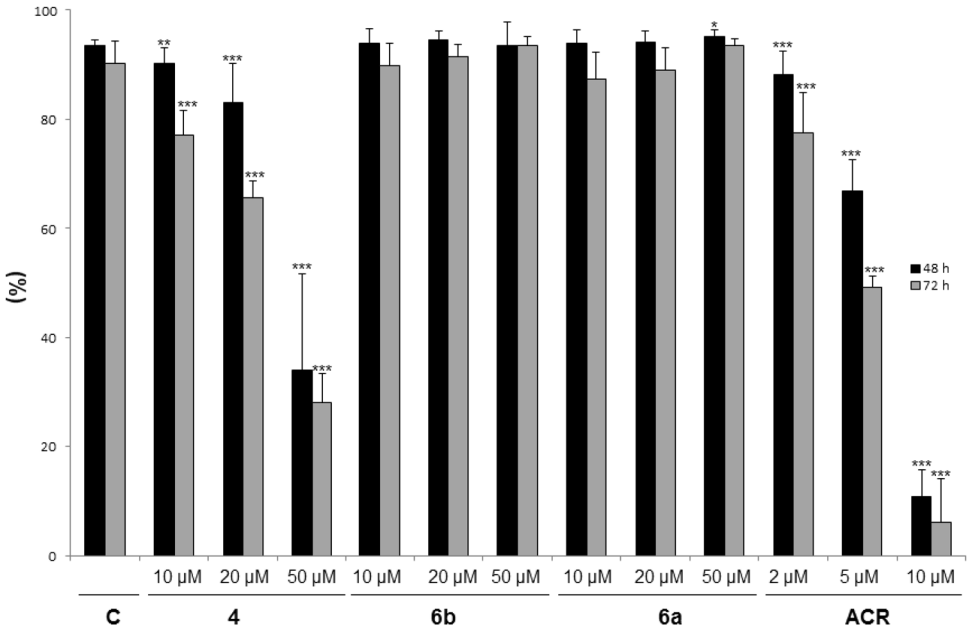

Fig. 8 The effect of acridine (ACR, positive control, 2–10 × 10^{-6} M) and derivatives **4**, **6a**, and **6b** (10–50 × 10^{-6} M) on changes in viability 48 and 72 h after treatment. The results are presented as a mean ± SD, statistical significance: $p < 0.05$ (*), $p < 0.01$ (**), $p < 0.005$ (***) for each experimental group compared to untreated control (C)

targets candidates for development as new topo I inhibitors (Basili et al. 2008; Bera et al. 2008).

Cytotoxic studies

While considerable research has focused on the development of acridine derivatives as potential anti-cancer agents, the highly cytotoxic nature of the compounds has limited their clinical application to very specific uses. For example, 9-anilino acridine derivatives (Su et al. 2006) exhibited potent in vitro cytotoxicity against human lymphoblastic leukemia cells (CCRF-CEM), or 3,4-dihydro-1*H*-[1,3]oxazino[4,5-c] acridines (Ouberai et al. 2006) were characterized with cytotoxic activity against HT-29 colon adenocarcinoma cell line. In this study, we also investigated the effectiveness of new acridine derivatives **4**, **6a**, and **6b** on the HL-60 human promyelocytic leukemia cell line using various flow cytometer techniques.

The effect of derivatives **4**, **6a**, and **6b** on the metabolic activity of HL-60 cells was determined by examining the number of MTT metabolizing cells and their metabolic potency after treatment with varying concentrations of the

studied derivatives (0–100 × 10^{-6} M) over 24, 48, or 72 h. The results show that the studied derivatives had a dose-dependent and time-dependent inhibitory effect on the metabolic activity of HL-60 cells; the effect was relatively weak at lower concentrations and over shorter time periods, but at concentrations greater than 20 × 10^{-6} M after 72 h incubation the effect was markedly stronger (Fig. 6).

Table 2 IC_{50} values for the MMP and viability evaluated 48 and 72 h after treatment with acridine (ACR) and derivatives **4**, **6a**, and **6b**

TMRE IC_{50} (μM)	48 h	72 h	PI IC_{50} (μM)	48 h	72 h
4	31.58	30.58	**4**	36.15	27.85
6a	nd	nd	**6a**	nd	nd
6b	nd	nd	**6b**	nd	nd
ACR	6.37	5.23	ACR	6.40	5.04

TMRE tetramethylrhodamine ethyl ester, *PI* propidium iodide

Further tests were then performed in order to determine whether the cytotoxic effects of the studied derivatives can be related to the changes in the MMP, the mechanism implicated in cell death and in the interference of the cell cycle progression.

Cell death can be activated by a mitochondria-dependent apoptotic process, which includes the opening of mitochondrial permeability transition complex pore, mitochondrial transmembrane potential dissipation, and other factors.

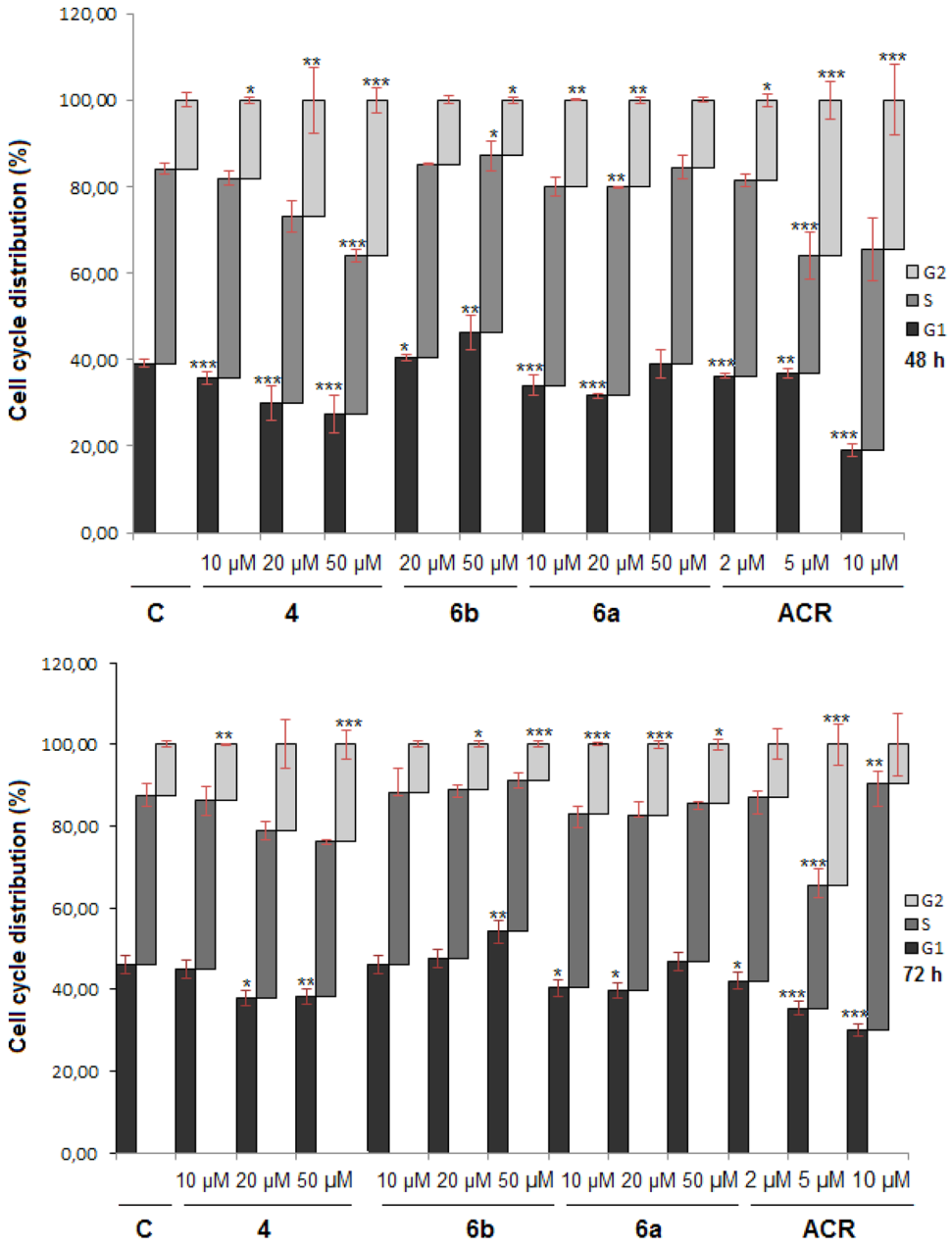

Fig. 9 The effect of acridine (ACR, positive control, 2–10 × 10^{-6} M) and derivatives **4**, **6a**, and **6b** (10–50 × 10^{-6} M) on cell cycle distribution 48 and 72 h after treatment. The results are presented as a mean ± SD, statistical significance: $p < 0.05$ (*), $p < 0.01$ (**), $p < 0.005$ (***) for each experimental group compared to untreated control (C)

MMP is lost during the process of apoptosis through the disruption of energy metabolism (Salem et al. 2016), therefore we decided to investigate the rate of MMP dissipation induced by derivatives **4**, **6a**, and **6b** (Fig. 7). Derivative **4** caused a significant reduction in the MMP of HL-60 cells after 72-h treatment at a concentration of at 50 μM. Treatment with derivatives **6a** and **6b** had a weaker effect on the MMP in comparison to that recorded for the positive control, acridine. The analysis of cell viability revealed similar results as that of the MMP analysis. Derivative **4** and the acridine control were more effective than derivatives **6a** and **6b** (Fig. 8). IC_{50} values were also calculated for both techniques (MMP and viability) and for different time points (Table 2).

As can be seen in Fig. 9, a significant increase in the number of cells in the G1 phase of cell cycle was observed following 48-h exposure to 10, 20, and 50 μM of derivatives **4** and **6a** and the acridine control. Moreover, derivatives **4** and **6b** caused a reduction of cells in the S phase at 50 μM. A corresponding increase in the cell population in the G2 phase of cell cycle was also observed after 48-h exposure to 50 μM of derivatives **4** and the acridine control. Similar results were obtained following the incubation of HL-60 cells with 10, 20, and 50 μM of the studied derivatives for 72 h. Derivative **4** had a clear effect on cell cycle distribution, visible as an increased proportion of cells in the G2 phase with a simultaneous reduction in the number of cells in the G1 phase.

Conclusion

In this study, a series of new acridine derivatives, compounds **4**, **6a**, and **6b** was synthesized and investigated. The compounds showed evidence of DNA-binding activity and the binding constants, *K*, of the ligands were calculated to be 3.5×10^4–$4.0 \times 10^4\ M^{-1}$. The results of UV–Vis, fluorescence spectroscopy, LD spectropolarimetry, DNA melting techniques, and viscometry all indicate that the studied compounds act as effective DNA-binding agents. The studied compounds were also investigated for their inhibitory effect on topo I (inhibitory activity at 60 μM). The biological activities of the derivatives were studied using MTT assay and flow cytometric methods after 24 and 48 h incubation with human HL-60 leukemic cancer cell line. The results from the MTT assay showed that the studied acridine derivatives had a dose-dependent and time-dependent inhibitory effect on the metabolic activity of HL-60 cells. An anti-tumor activity toward selected cell line, IC_{50}, reached μM levels for the most active substance **4**, allowing to consider it to be interesting from point of further testing. Cytotoxicity against HL-60 cells of the most potent derivative **4** (27.85 μM, 72 h) is several times lower than that of model amsacrine ($IC_{50} = 0.34$ μM).

Our results obtained from this work identify various areas of valuable information relating to ligand–DNA interactions, which could be useful for rational drug design and helpful in the development of their potential pharmaceutical and biological effect.

Acknowledgements This study was supported by Slovak Research and Development Agency under contract VVCE-0001-07, VEGA grants No. 1/0001/13, and 1/0672/11 and MH CZ-DRO (UHHK, 00179906). The authors would like to thank Jana Kašpárkova and Viktor Brabec for their advice on LD measurement and viscometric techniques.

Compliance with ethical standards

Conflict of interest The authors declare that they have no competing interests.

References

Barros FW, Silva TG, da Rocha Pitta MG, Bezerra DP, Costa-Lotufo LV, de Moraes MO, Pessoa C, de Moura MA, de Abreu FC, de Lima Mdo C, Galdino SL, Pitta Ida R, Goulart MO (2012) Synthesis and cytotoxic activity of new acridine-thiazolidine derivatives. Bioorg Med Chem 20:3533–3539

Barros FW, Bezerra DP, Ferreira PM, Cavalcanti BC, Silva TG, Pitta MG, de Lima Mdo C, Galdino SL, Pitta Ida R, Costa-Lotufo LV, Moraes MO, Burbano RR, Guecheva TN, Henriques JA, Pessoa C (2013) Inhibition of DNA topoisomerase I activity and induction of apoptosis by thiazacridine derivatives. Toxicol Appl Pharmacol 268:37–46

Basili S, Basso G, Faccio A, Granzhan A, Ihmels H, Moro S, Viola G (2008) Diazoniapolycyclic ions inhibit the activity of topoisomerase I and the growth of certain tumor cell lines. ChemMedChem 31671:e1676

Bera R, Sahoo BK, Ghosh KS, Dasgupta S (2008) Studies on the interaction of isoxazol-curcumin with calf thymus DNA. Int J Biol Macromol 42:14–21

Busa J (2006) Octave. Technical University, Kosice

Cain BF, Baguley BC, Denny WA (1978) Potential antitumor agents. 28. Deoxyribonucleic acid polyintercalating agents. J Med Chem 21:658–668

Champoux JJ (2001) DNA topoisomerases: structure, function and mechanism. Ann Rev Biochem 70:369–413

Chitrapriya N, Jang YJ, Kim SK, Lee H (2011) Non-intercalative binding mode of bridged binuclear chiral Ru(II) complexes to native duplex DNA. J Inorg Biochem 105:1569–1575

Di Giorgio C, Nikoyan A, Decome L, Botta C, Robin M, Reboul J-P, Sabatier A-S, Matta A, De Méo M (2008) DNA-damaging activity and mutagenicity of 16 newly synthesized thiazolo[5,4-a] acridine derivatives with high photo-inducible cytotoxicity. Mut Res 650:104–114

Goodell JR, Ougolkov AV, Hiasa H, Kaur H, Remmel R, Billadeau DD, Ferguson DM (2008) Acridine-based agents with topoisomerase II activity inhibit pancreatic cancer cell proliferation and induce apoptosis. J Med Chem 51:179–182

Hannon MJ, Moreno V, Prieto MJ, Moldrheim E, Sletten E, Meistermann I, Isaac CJ, Sanders KJ, Rodger A (2001) Intramolecular

DNA coiling mediated by a metallo-supramolecular cylinder. Angew Chem Int Ed Engl 40:879–884

Ilis M, Bucos M, Dumitrascu F, Circu V (2011) Mesomorphic behaviour of N-benzoyl-N′-aryl thioureas liquid crystalline compounds. J Mol Struct 987:1–6

Janočková J, Plšíková J, Kašpárková J, Brabec V, Jendželovský R, Mikeš J, Kovaľ J, Hamuľaková S, Fedoročko P, Kuča K, Kožurková M (2015a) Inhibition of DNA topoisomerases I and II and growth inhibition of HL-60 cells by novel acridine-based compounds. Eur J Pharm Sci 76:192–202

Janočková J, Plšíková J, Kovaľ J, Jendželovský R, Mikeš J, Kašpárková J, Brabec V, Hamulaková S, Fedoročko P, Kožurková M (2015b) Tacrine derivatives as dual topoisomerase I and II catalytic inhibitors. Bioorg Chem 59:168–176

Jenkins TC (1997) Optical absorbance and fluorescence techniques for measuring DNA-drug interactions. In: Fox KR (ed) Drug-DNA interaction protocols. Human Press, Totowa, NJ, p 195. 218

Kamatchi TS, Chitrapriya N, Kim SK, Fronczek FR (2013) Influence of carboxylic acid functionalities in ruthenium(II) polypyridyl complexes on DNA binding, cytotoxicity and antioxidant activity: synthesis, structure and in vitro anticancer activity. Eur J Med Chem 59:253–264

Khan KM, Maharvi GM, Hayat S, Zia-Ullah, Choudhary MI, Atta-ur-Rahman (2003) An expedient esterification of aromatic carboxylic acids using sodium bromate and sodium hydrogen sulfite. Tetrahedron 59:5549–5554

Khurana JM, Chauhan S, Bansal G (2004) Facile hydrolysis of esters with KOH-methanol at ambient temperature. Monatshefte für Chemie 135:83–87

Lafayette EA, De Almeida SV, Da Rocha Pitta MG, Beltrao EIC, Da Silva TG, De Moura RO, Da Rocha Pitta I, De Carvalho Júnior LB, De Lima MDCA (2013) Synthesis, DNA binding and topoisomerase I inhibition activity of thizacridine and imidazacridine derivatives. Molecules 18:15035–15050

Lang X, Li L, Chen Y, Sun Q, Wu Q, Liu F, Tan C, Liu H, Gao C, Jiang Y (2013) Novel synthetic acridine derivatives as potent DNA-binding and apoptosis-inducing antitumor agents. Bioorg Med Chem 21:4170–4177

Li X, Ma D, Yang H, Tan G, Du H, Wang K, Zhang P, Chen H (2014) Synthesis, antitumor activity and DNA binding of acridine-polyamine conjugates. Chem J Chinese U 35:1181–1188

Li WY, Xu JG, Guo XQ, Zhu QZ, Zhao YB (1997) Study on the interaction between rivanol and DNA and its application to DNA assay. Spectrochim Acta A 53:781–787

Ling X, Zhong WY, Huang Q, Ni KY (2008) Spectroscopic studies on the interaction of pazufloxacin with calf thymus DNA. J Photochem Photobiol B 93:172–176

McGhee JD, von Hippel PH (1974) Theoretical aspects of DNA-protein interactions: co-operative and non-co-operative binding of large ligands to a one dimensional homogeneous lattice. J Mol Biol 86:469–489

Moukharskaya J, Verschraegen C (2012) Topoisomerase 1 inhibitors and cancer therapy. Hematol Oncol Clin North Am 26:507–525

Neyhart GA, Grover N, Smith SR, Kalsbeck WA, Fairley TA, Cory M, Thorp HH (1993) Binding and kinetics studies of oxidation of DNA by oxoruthenium(IV). J Am Chem Soc 115:4423–4428

Ouberai M, Asche C, Carrez D, Croisy A, Dumy P, Demeunynck M (2006) 3,4-Dihydro-1H-[1,3]oxazino[4,5-c]acridines as a new family of cytotoxic drugs. Bioorg Med Chem Lett 16:4641–4643

Patel DJ (1979) Nuclear magnetic resonance studies of drug-nucleic acid interactions at the synthetic DNA level in solution. Acc Chem Res 12:118–125

Phelps C, Lee W, Jose D, von Hippel PH, Marcus AH (2013) Single-molecule FRET and linear dichroism studies of DNA breathing and helicase binding at replication fork junction. Proc Natl Acad Sci USA 110:17320–17325

Rajendran A, Nair BU (2006) Unprecedented dual binding behaviour of acridine group of dye: a combined experimental and theoretical investigation for the development of anticancer chemotherapeutic agents. Biochim Biophys Acta 1760:1794–1801

Ramalinga K, Vijayalakshmi P, Kaimal TNB (2002) A mild and efficient method for esterification and transesterification catalyzed by iodine. Tetrahedron Lett 43:879–882

Rehman SU, Yaseen Z, Husain MA, Sarwar T, Ishqi HM, Tabish M (2014) Interaction of 6 mercaptopurine with calf thymus DNA—deciphering the binding mode and photoinduced DNA damage. PLoS ONE 9:e93913

Salem O, Vilkova M, Plsikova J, Grolmusova A, Burikova M, Prokaiova M, Paulikova H, Imrich J, Kozurkova M (2015) DNA binding, anti-tumour activity and reactivity toward cell thiols of acridin-9-ylalkenoic derivatives. J Chem Sci 127:931–940

Salem OM, Vilková M, Janočková J, Jendželovský R, Fedoročko P, Žilecká E, Kašpárková J, Brabec V, Kožurková M (2016) New spiro tria(thia)zolidine-acridines as topoisomerase inhibitors, DNA binders and cytostatic compounds. Int J Biol Macromol 86:690–700

Su T-L, Lin Y-W, Chou T-C, Zhang X, Bacherikov VA, Chen C-H, Liu LF, Tsai TJ (2006) Potent antitumor 9-anilinoacridines and acridines bearing an alkylating N-mustard residue on the acridine chromophore: synthesis and biological activity. J Med Chem 49:3710–3718

Terenzi A, Ducani C, Male L, Barone G, Hannon MJ (2013) DNA interaction of CuII, NiII and ZnII functionalized salphen complexes: studies by linear dichroism, gel electrophoresis and PCR. Dalton Trans 42:11220–11226

Tsukamoto I, Koshio H, Kuramochi T, Saitoh C, Yanai-Inamura H, Kitada-Nozawa C, Yamamoto E, Yatsu T, Shimada Y, Sakamoto S, Tsukamoto S (2009) Synthesis and structure–activity relationships of amide derivatives of (4,4-difluoro-1,2,3,4-tetrahydro-5*H*-1-benzazepin-5-ylidene)acetic acid as selective arginine vasopressin V_2 receptor agonists. Bioorg Med Chem 17:3130–3141

Ungvarská Maľučká L, Vilková M, Kožíšek J, Imrich J (2016) Strong deshielding in aromatic isoxazolines. Magn Reson Chem 54:17–27

Vantova Z, Paulikova H, Sabolova D, Kozurkova M, Suchanova M, Janovec L, Kristian P, Imrich J (2009) Cytotoxic activity of acridin-3,6-diyl dithiourea hydrochlorides in human leukemia line HL-60 and resistant subline HL-60/ADR. Int J Biol Macromol 45:174–180

Vilková M, Ungvarská Maľučká L, Imrich J (2016) Prediction by ^{13}C NMR of regioselectivity in 1,3-dipolar cycloadditions of acridin-9-yl dipolarophiles. Magn Reson Chem 54:8–16

Vos SM, Tretter EM, Schmidt BH, Berger JM (2011) All tangled up: how cells direct manages and exploits topoisomerase function. Nature Rev 12:827–841

Yao B-L, Mai Y-W, Chen S-B, Xie H-T, Yao P-F, Ou T-M, Tan J-H, Wang H-G, Li D, Huang S-L, Gu L-Q, Huang Z-S (2015) Design, synthesis and biological evaluation of novel 7-alkylamino substituted benzo[a]phenazin derivatives as dual topoisomerase I/II inhibitors. Bioorg Med Chem 92:540–553